Functional Roles of the L-type Calcium Channel on Cardiac Pacemaking – Insights from Bifurcation Analysis

Jihong Liu[1], Jian Yu[2], Henggui Zhang[2,3]

[1]College of Information Science and Engineering, Northeastern University, Shengyang, China
[2]Biological Physics Group, School of Physics & Astronomy, The University of Manchester, UK
[3]School of Computer Science & Technology, Harbin Institute of Technology, China

Abstract

In this study, we used the bifurcation analysis technique to study the functional roles of the maximal channel conductace of the L-type calcium channel coded by isoforms of Cav1.2 and Cav1.3 in a novel mathematical model of murine sinoatrial node (SAN) cells. A continuous variation in the maximal channel conductance of I_{CaL} ($g_{CaL,1.2}$ and $g_{CaL,1.3}$) was carried out to reveal the emergence and annihilation of pacemaking action potentials (APs), changes in AP's cycle length, maximal diastolic potential and overshoot. Parameter value range of the channel conductances essential for generating or annihilating pacemaking APs were identified. Our data demonstrates that the L-type calcium channel current contributes to cardiac pacemaking APs, especially during their diastolic and up-stroke depolarization phases.

1. Introduction

The initiation and control of the heart excitation rhythm is controlled by a special region of the heart, the sinoatrial node (SAN), cells of which generate spontaneous and rhythmic electrical action potentials (APs) [1]. Though a larger amount of experimental data have been obtained from voltage-clamp experimentations about the kinetics of ion channels of the SAN cells responsible for producing auto-rhythmic and spontaneous pacemaking APs, the specific role of each of the individual ion channels in generating cardiac pacemaking APs is not completely understood yet [1-2].

Bifurcation analysis [3-6] provides a useful tool to analyse parameter-dependent functions of a biological system, and therefore, can be used to elucidate the functional role of individual ion channels in contributions to APs of cardiac models [7-16]. So far several tools have been developed for bifurcation analysis, and have been applied to cardiac cell models. In cardiac models like atrial and ventricular cells, bifurcation analysis has assisted in understanding the ionic mechanisms underlying the genesis of pro-arrythmogenic early-after-depolarization, delayed-after-depolarization and spontaneous release of $[Ca^{2+}]_i$ leading to erratic wave propagations in cardiac tissues [7-8]. In cardiac models of pacemaking SAN cells, bifurcation analyse has also been used to obtain insights into the mechanisms of cardiac pacemaking activities [11-16]. In mathematical models, it has been shown that various parameters of the models, and in particular ion channel conductances, have considerable effects on modulating the characteristics of pacemaking APs, such as the cycle length (CL; the time interval between two successive APs), the maximal diastolic potential (MDP) and overshoot (OS). A bifurcation analysis helps to reveal the influence of individual ion channels on pacemaking activities.

The aim of this study was to use one-parameter-bifurcation analysis to study the functional roles of the maximal channel conductances of the L-type Ca^{2+} channels coded by isoforms of Cav1.2 ($I_{CaL,1.2}$) and Cav1.3 ($I_{CaL,1.3}$) on murine pacemaking APs. To this end, a continuous variation in the maximal channel conductances of I_{CaL} ($g_{CaL,1.2}$ and $g_{CaL,1.3}$) was carried out in the bifurcation analysis, to evaluate the functional role of I_{CaL} on the emergence and annihilation of pacemaking APs, and its impacts on modulating AP's CL, MDP and OS. Parameter value ranges of the $g_{CaL,1.2}$ and the $g_{CaL,1.3}$ essential for generating and/or annihilating pacemaking activity were identified.

2. Methods

A mathematical model for the electrical APs of central murine SAN node cells developed by Kharche *et al*. [17] was used for this study. The model was based on and validated against experimental data obtained from murine SAN cells at ionic channel and cellular AP levels, and incorporated molecular bases for pacemaking APs [18,19]. Recently, it has been improved to incorporate comprehensive pacemaking mechanisms of the "membrane clock" and "Ca^{2+} clock" mechanisms [20]. With the model [17], we implemented the well-

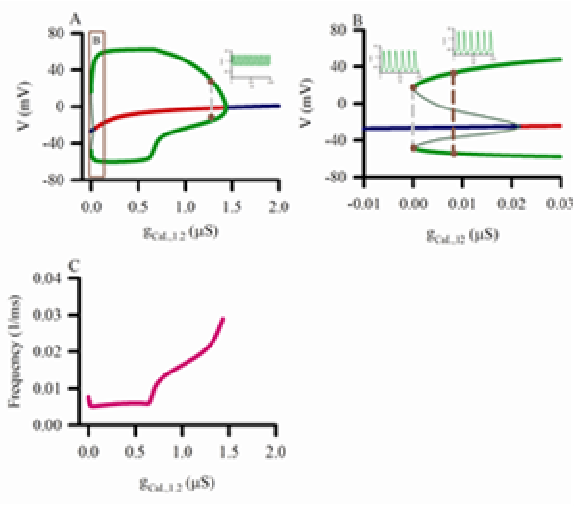

Figure 1. Bifurcation structure for parameter $g_{CaL,1.2}$. (A) Bifurcation structure of $g_{CaL,1.2}$. Different system states are demonstrated by different color lines: stable steady state (blue line), unstable steady state (red line), stable oscillation state (thick green line), unstable oscillation line (thin dark green line). The inset shows the AP of the state marked by dark red points. (B) Enlarged region marked by a dark red box in (A). Insets show the AP marked by dark red points. (C) Frequency of the oscillation state shown in (A) when $g_{CaL,1.2}$ is varied.

established continuation algorithms embedded in AUTO [3-7] to compute the steady state, bifurcation point, and bifurcation branches of the solutions of the model with the maximal channel conductances of $I_{CaL,1.2}$ ($g_{CaL,1.2}$) and $I_{CaL,1.3}$ ($g_{CaL,1.3}$) being continuously varied. As the Kharche et al. model of murine central SAN cell [17] contains $[Ca^{2+}]_i$ handling mechanism that are much slower as compared to the ionic channel kinetics and the time course of membrane APs, in numerical experimentations, we have removed the slow $[Ca^{2+}]_i$ handling mechanisms from the model because the continuation algorithms require the initial state of the model to be highly stable or highly periodic. Therefore, in the model, we set the ionic concentrations of $[Ca^{2+}]_i$ to a constant value of 100 nM. It is of note that such modifications did not alter significantly the characteristics of the simulated APs.

3. Results

Figure 1 presents the results of bifurcation analysis of the model associated with a continuous variation of the parameter value of $g_{CaL,1.2}$. As experimental data suggests that the normal physiological value of $g_{CaL,1.2}$ in the central murine SAN cells is around $0.8x10^{-2}$ μS, therefore, in the bifurcation analysis, $g_{CaL,1.2}$ was varied in a range from 0 to 2.0 μS. Figure 1A illustrates the traced bifurcation cascades for the whole parameter range of $g_{CaL,1.2}$ (0 – 2.0 μS), while Figure 1B highlights the local bifurcation structure with $g_{CaL,1.2}$ being around the vicinity of its normal physiological value (i.e., around $0.8x10^{-2}$ μS; the points that connected by dark red dashed line in Figure 1B). Our results show that the bifurcation begins at $0.2x10^{-2}$ μS, which enabling the model to transfer from a steady state to a stable oscillation state. The oscillation state terminates at 1.44 μS (Figure 1A), enabling the model to transfer from a stable oscillation state back to a stable steady state. With $g_{CaL,1.2}$ greater than the bifurcation point ($0.2x10^{-2}$ μS), an increase of $g_{CaL,1.2}$ is first accompanied by a decrease in the oscillation frequency of the model solution (*i.e.*, a decrease in the pacing rate of APs), but then followed by an increase in the oscillation frequency as shown in Figure 1C. This is attributable to the fact that I_{CaL} is a primary factor that contributes to both of the upstroke velocity of pacemaking APs and the duration of the AP (APD). With an increase in $g_{CaL,1.2}$, there is an increase in both of the upstroke velocity and the APD. While the former tends to speed up the pacemaking rate, but the effect of the latter is to slow it down. A complicate interaction between the two processes determines whether the pacemaking rate is increased or decreased. When the value of $g_{CaL,1.2}$ is greater than 1.5 μS, the model solution reaches to a quiescent state, indicating a transition of the model solution from a limit cycle (LC) state to a stable steady state. This may be attributable to the imbalance between the depolarizing inward current provided by I_{CaL} and the repolarizing outward current provided by potassium channels. As a result, the amplitude of AP gradually decreases while the maximal diastolic potential is elevated. An elevation in the maximal diastolic potential inhibits a fully complete activation of $I_{Ca,L}$, which contributes to the dumping oscillation of the model solution, leading to a stable steady state.

Around the left Hopf bifurcation (HB) point (*i.e.*, the lower HB point), the bifurcation structure shows bi-stability (*i.e.*, in the range of $g_{CaL,1.2}$ from $0.2x10^{-4}$ μS to $0.2x10^{-1}$ μS, Figure 1A and B). This suggests that if $g_{CaL,1.2}$ falls into this value range, the system will be in stable steady state or in a stable oscillation state, purely depending on the initial conditions of the state variables of the model. This is the feature of subcritical HB process. In such a case, if a strong enough perturbation is applied to the model, the model may transfer from a steady-state to a LC state, or vice versa. It is of note that this parameter range is close to the physiological value of $g_{CaL,1.2}$, indicating the functional impacts of an external disturbance on modulating cardiac pacemaking APs. Around the right HB point (*i.e.*, the higher HB point), the bifurcation structure does not show such a bi-stability, but with the feature of a super-critical HB process. When the value of $g_{CaL,1.2}$ is around this region, the system will remain in a stable oscillation state or a stable steady state and the model solution is insensitive to a small perturbation.

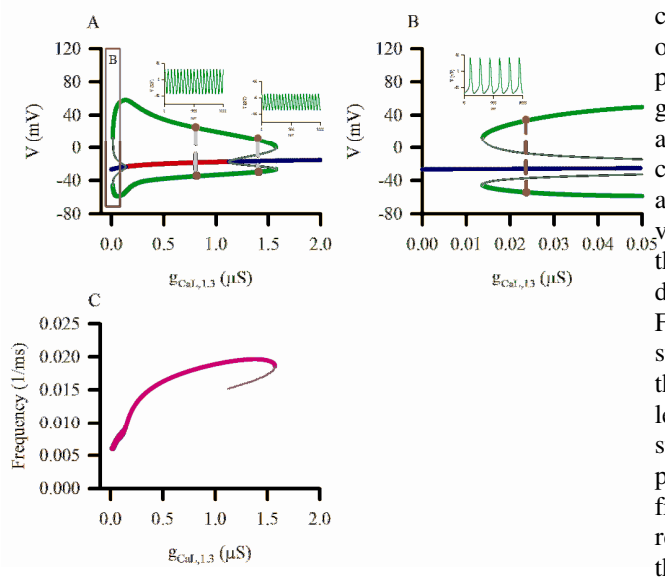

Figure 2. Bifurcation structure for parameter $g_{CaL,1.3}$. (A) Traced bifurcation structure with a continuous variation of $g_{CaL,1.3}$. Different system states are demarcated by different color lines: stable steady state (blue line), unstable steady state (red line), stable oscillation state (thick green line), unstable oscillation line (thin dark green line). The inset shows the AP of the state marked by dark red points. (B) Enlarged parameter region marked by the dark red box in (A). Insets show the AP marked by dark red points. (C) Frequency of the oscillation state shown in (A). Thick green line presents stable oscillation, and thin dark green line presents unstable oscillation.

Similar bifurcation analyses were also performed to elucidate the functional role of $g_{CaL,1.3}$ on modulating the pacemaking APs. Results are shown in Figure 2. As experimental data suggests that the physiological value of $g_{CaL,1.3}$ in the central murine SAN cells is around $0.2x10^{-2}$ μS, therefore, in numerical experimentations, $g_{CaL,1.3}$ was varied between a value range of 0 – 2.0 μS. Figure 2A shows the traced bifurcation cascades with a continuous change of $g_{CaL,1.3}$, and Figure 2B highlights the bifurcation structure with the value of $g_{CaL,1.3}$ being at the vicinity of a normal physiological value (the points marked by dark red dashed line in Figure 2B). Our data show that the bifurcation begins at $g_{CaL,1.3}$=0.136 μS, marking the point for the system to transfer from a stable steady state to a stable oscillation state. However, the oscillation solution terminates at $g_{CaL,1.3}$=1.123 μS. At this point the model solution transfers from a stable oscillatory solution to a stable steady state (see Figure 2A). During the parameter range of 0.136 - 1.123 μS, an increase in $g_{CaL,1.3}$ is accompanied by an increase in the frequency of the oscillatory solution, indicating the acceleration of the pacemaking activity (Figure 2C). This confirms the important role of I_{CaL} coded by Cav1.3 as one of the primary factors contributing to the genesis of pacemaking APs. It is also shown that with an increase of $g_{CaL,1.3}$, the amplitude of AP gradually decreases. This is attributable to the elevation of the MDP (similar to the case when $g_{CaL,1.2}$ is increased), that inhibits the full activation of I_{CaL}, resulting in a decrease in the upstroke velocity of APs and therefore their amplitudes. However, the higher (i.e, the right) HB point of $g_{CaL,1.3}$ is dramatically different to that of the $g_{CaL,1.2}$. As shown in Figure 2A, the right HB point of the $g_{CaL,1.3}$ bifurcation structure is subcritical, rather than that of super-critical of the $g_{CaL,1.2}$ bifurcation structure. Therefore, at both of the left and right HB points of the $g_{CaL,1.3}$ bifurcation structure, the model solution is bi-stable. The identified parameter range of $g_{CaL,1.3}$ for the left bi-stability region is from 0.0137 μS to 0.136 μS; and for the right bi-stability region is from 1.123 μS to 1.572 μS (see the dark green thin line in Figure 2A and B). Thus the normal physiology value of $g_{CaL,1.3}$ (0.0237 μS) is within the left bi-stability regionFigures can fit across both columns if necessary.

4. Conclusions

In this study, we have used bifurcation analysis techniques to study the functional role of $g_{CaL,1.2}$ and $g_{CaL,1.3}$ in cardiac pacemaking APs. Our results show that, though coded by distinctive isoforms, both types of I_{CaL} (i.e., $I_{CaL,1.2}$ and $I_{CaL,1.3}$) plays important roles in generating cardiac pacemaking APs. Our mathematical analysing results are consistent with experimental data, which shows that blocking I_{CaL} by pharmacological agents abolishes pacemaking APs [1, 17,18].

However, our findings also show that the functional roles of $I_{CaL,1.2}$ and $I_{CaL,1.3}$ are different. From the bifurcation analysis, it is shown that $I_{CaL,1.3}$ contributes to diastolic depolarization. Reducing $I_{CaL,1.3}$ slows down the diastolic depolarization, leading to a marked negative chronotropic effect. However, $I_{CaL,1.2}$ contributes to the upstroke of AP, and provides depolarization current maintaining the AP plateau during the repolarization phases. Reducing $I_{CaL,1.2}$ produces a reduced maximal upstroke velocity and OS of APs. It also abbreviates the APD of APs.

The functional differences between $I_{CaL,1.3}$ and $I_{CaL,1.2}$ may be attributable to their distinctive channel properties [18,19]. It has been shown that $I_{CaL,1.3}$ activates at more negative membrane potential and also has more negative steady-state activation (by ~ 15 mV) and inactivation (by ~ 10 mV) in respect to $I_{CaL,1.2}$. The measured activation threshold potential of $I_{CaL,1.3}$ is about ~ -50 mV and peaks at -10 mV, which are more negative than those of $I_{CaL,1.2}$ (activation threshold: -20 mV; I-V peak: +10 mV). As $I_{CaL,1.3}$ has a low activation threshold, which falls in the potential range of diastolic depolarisation phase, its

activation provides an important component of depolarizing current modulating pacemaking rates. However $I_{CaL,1.2}$ has a high activation threshold, which falls in the range of AP during the upstroke and the following repolarization phases, thus its activation provides a depolarizing current modulating the overshoot and sustaining the plateau of the action potential. The simulation results provide a solid evidence to support the hypothesis that $I_{CaL,1.3}$ and $I_{CaL,1.2}$ are functionally different in generating and controlling cardiac rhythms due to their distinctive channel kinetics and properties.

Acknowledgements

This work is supported by grants from National Science Foundations of China (NSFC 61001167; NSFC 61173086; NSFC 61179009).

References

[1] Boyett MR, Dobrzynski H, Lancaster MK, Jones SA, Honjo H & Kodama I. (2003). Sophisticated architecture is required for the sinoatrial node to perform its normal pacemaker function. J Cardiovasc Electrophysiol 14, 104-106.

[2] Lakatta EG, Vinogradova TM & Maltsev VA. (2008). The missing link in the mystery of normal automaticity of cardiac pacemaker cells. *Ann N Y Acad Sci* **1123,** 41-57.

[3] Chickarmane V, Paladugu SR, Bergmann F & Sauro HM. (2005). Bifurcation discovery tool. Bioinformatics 21, 3688-3690.

[4] Schmidt H & Jirstrand M. (2006). Systems Biology Toolbox for MATLAB: a computational platform for research in systems biology. Bioinformatics 22, 514-515.

[5] Ermentrout B. (2002). Simulating, analyzing, and animating dynamical systems: a guide to XPPAUT for researchers and students. Society for Industrial and Applied Mathematics, Philadelphia.

[6] Dhooge A, Govaerts W & Kuznetsov YA. (2003). Numerical continuation of fold bifurcations of limit cycles in MATCONT, vol. 2657. Springer Berlin, Heidelberg.

[7] Benson AP, Clayton RH, Holden AV, Kharche S & Tong WC. (2006). Endogenous driving and synchronization in cardiac and uterine virtual tissues: bifurcations and local coupling. Philos Transact A Math Phys Eng Sci 364, 1313-1327.

[8] Landau M, Lorente P, Michaels D & Jalife J. (1990). Bistabilities and annihilation phenomena in electrophysiological cardiac models. Circ Res 66, 1658-1672.

[9] Vinet A & Roberge FA. (1990). A model study of stability and oscillations in the myocardial cell membrane. J Theor Biol 147, 377-412.

[10] Faber GM, Silva J, Livshitz L & Rudy Y. (2007). Kinetic properties of the cardiac L-type Ca2+ channel and its role in myocyte electrophysiology: a theoretical investigation. Biophys J 92, 1522-1543.

[11] Tong WC & Holden AV. (2006). Bifurcation analysis of genetically engineered pacemaking in mammalian heart. *J Biol Phys* **32** 169-172.

[12] Chay TR & Lee YS. (1992). Studies on re-entrant arrhythmias and ectopic beats in excitable tissues by bifurcation analyses. J Theor Biol 155, 137-171.

[13] Kurata Y, Hisatome I, Imanishi S & Shibamoto T. (2002). Dynamical description of sinoatrial node pacemaking: improved mathematical model for primary pacemaker cell. Am J Physiol Heart Circ Physiol 283, H2074-2101.

[14] Kurata Y, Hisatome I, Imanishi S & Shibamoto T. (2003). Roles of L-type Ca2+ and delayed-rectifier K+ currents in sinoatrial node pacemaking: insights from stability and bifurcation analyses of a mathematical model. Am J Physiol Heart Circ Physiol 285, H2804-2819.

[15] Kurata Y, Hisatome I, Matsuda H & Shibamoto T. (2005). Dynamical mechanisms of pacemaker generation in IK1-downregulated human ventricular myocytes: insights from bifurcation analyses of a mathematical model. Biophys J 89, 2865-2887.

[16] Kurata Y, Matsuda H, Hisatome I & Shibamoto T. (2008). Regional difference in dynamical property of sinoatrial node pacemaking: role of na+ channel current. Biophys J 95, 951-977.

[17] Kharche S, Higham J, Lei M, Zhang H. (2010). Functional role of ionic currents in a membrane delimited mouse cardiac pacemaking cells. Computing in Cardiology 37: 421-424.

[18] Mangoni ME, Couette B, Bourinet E, Platzer J, Reimer D, Striessnig J & Nargeot J. (2003). Functional role of L-type Cav1.3 Ca2+ channels in cardiac pacemaker activity. Proc Natl Acad Sci U S A **100,** 5543-5548.

[19] Masumiya H, Yamamoto H, Hemberger M, Tanaka H, Shigenobu K, Chen SR & Furukawa T. (2003). The mouse sino-atrial node expresses both the type 2 and type 3 Ca(2+) release channels/ryanodine receptors. FEBS Lett 553, 141-144.

[20] Kharche S, Yu J, Zhang H & Lei M. (2011). A Mathematical Model of Action Potentials of Mouse Sinoatrial Node Cells with Molecular Bases. Am J Physiology (Heart & Circulation) **301**: H945-63.

Address for correspondence.

Henggui Zhang
Biological Physics Group
School of Physics & Astronomy
The University of Manchester, Manchester, UK
henggui.zhang@manchester.ac.uk